PNAS
www.pnas.org

Supplementary Information for

A long non-coding RNA influences the choice of the X chromosome to be inactivated

Andreas Hierholzer [a,1], Corinne Chureau [b], Alessandra Liverziani [a], Nerea Blanes Ruiz [c], Bruce M. Cattanach [d], Alexander N. Young [a,2], Manish Kumar [a,3], Andrea Cerase [a,4] and Phil Avner [a,5]

[a] Epigenetics and Neurobiology Unit, EMBL Rome, Monterotondo, 00015, Italy; [b] Genomics and Epigenomics of Animal Development, Developmental and Stem Cell Biology Department, Institut Pasteur, 75015 Paris, France; [c] Blizard Institute, Barts and The London School of Medicine and Dentistry, Queen Mary University of London, London, E1 2AT, United Kingdom; and [d] MRC Mammalian Genetics Unit, Harwell Science and Innovation Campus, Oxfordshire OX11 0RD, United Kingdom

Present address: [1] Department of Biosystems Science and Engineering, ETH Zurich, 4058 Basel, Switzerland. [2] Present address: Blizard Institute, Barts and The London School of Medicine and Dentistry, Queen Mary University of London, London, E1 2AT, United Kingdom. [3] Present address: Department of Neurosurgery, Medical College of Georgia, Augusta University, 30912 Augusta, GA, USA. [4] Present address: Department of Biology, Università di Pisa, Pisa, Italy.

[5]corresponding author: Phil Avner

Email: philip.avner@embl.it

This PDF file includes:

Supplemental Figures S1 to S6

SI Methods

Supplementary Table

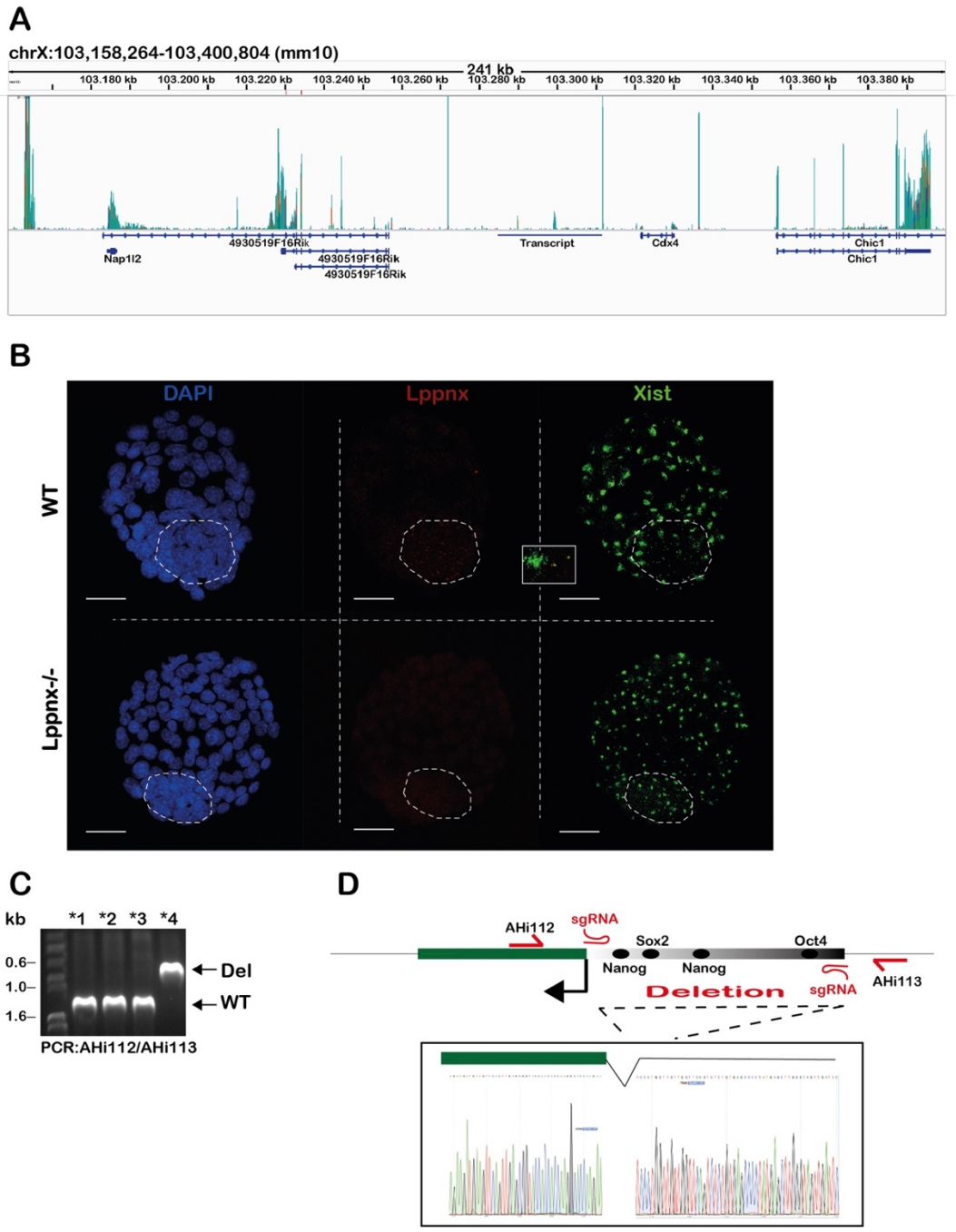

Fig. S1. The predicted X controlling element region harbours an uncharacterised transcript. RNA-seq analysis of female ES cells showing an uncharacterized transcript in the predicted Xce region (A). RNA-FISH analysis of mouse blastocysts shows the expression of this transcript in cells of the ICM (marked with a dashed line) after reactivation of the paternal X in WT embryos. The rectangular white box shows a close up of the co-localisation of the transcript and Xist in the ICM. (B. upper panel). Depletion of the putative promoter region of the transcript, named Lppnx) abolishes its expression in the ICM (B, lower panel). PCR based analysis, using primer pair AHi112/113 followed by sequence validation to identify the correct deletion in the founder line #4 (C, D).

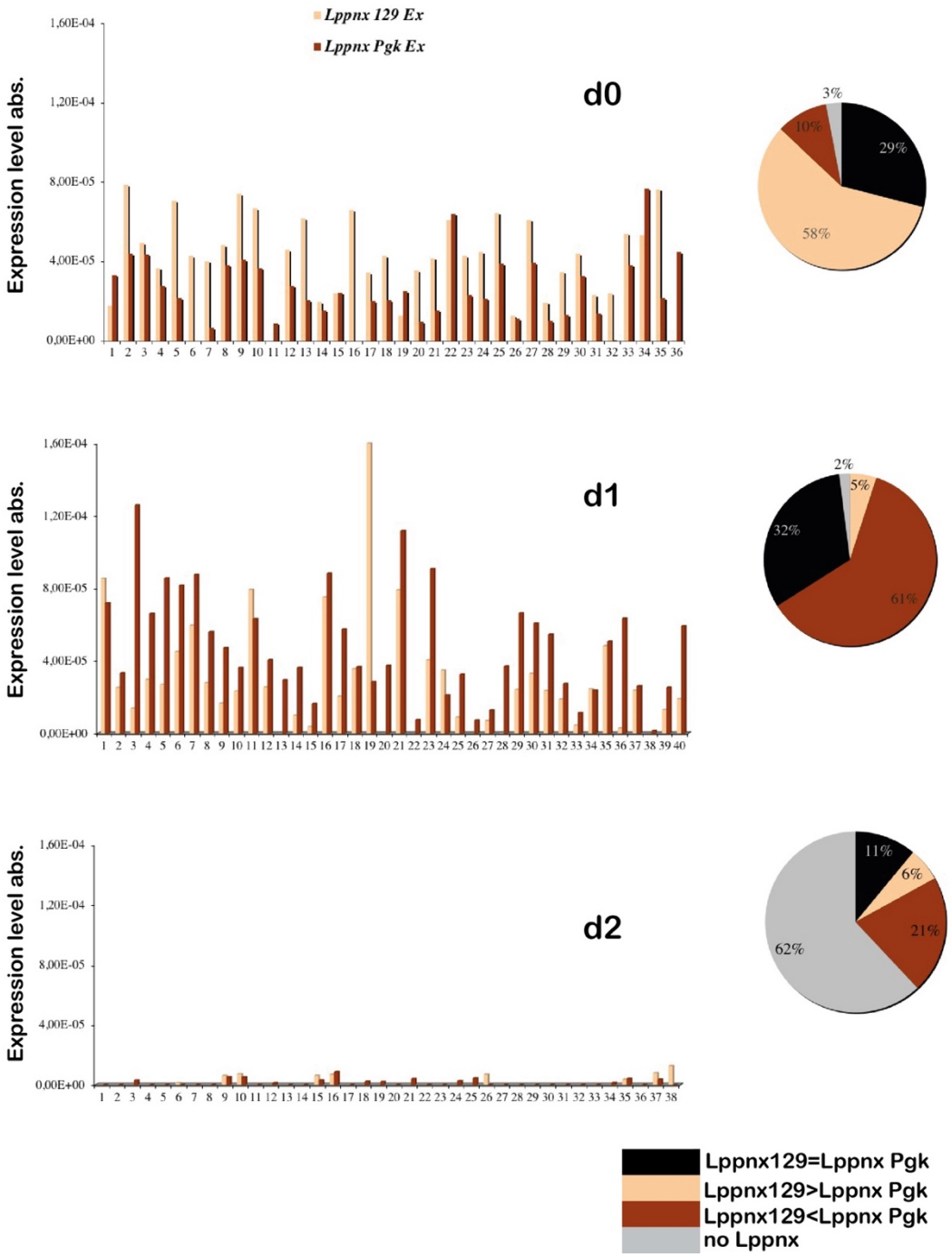

Fig. S2. Lppnx is differentially expressed from both alleles in female ES cells depending on background and timepoint of differentiation. Single cell qRT-PCR was performed on heterozygous Xce^a/Xce^c female ES cells using allele specific primers to analyse the allele specific expression of Lppnx. In undifferentiated ES cells Lppnx is expressed from both alleles, Xce^a and Xce^c. However, 58% of the analysed cells (in total 36 cells) show higher levels from the 129Sv (Xce^a) allele compared to 29% exhibiting higher expression from the Pgk1a (Xce^c) allele. This ratio is almost completely reversed at d1 of differentiation with ratios of 32% to 61% (in total 40 cells). At d2 almost all cells have silenced their Lppnx expression from both alleles.

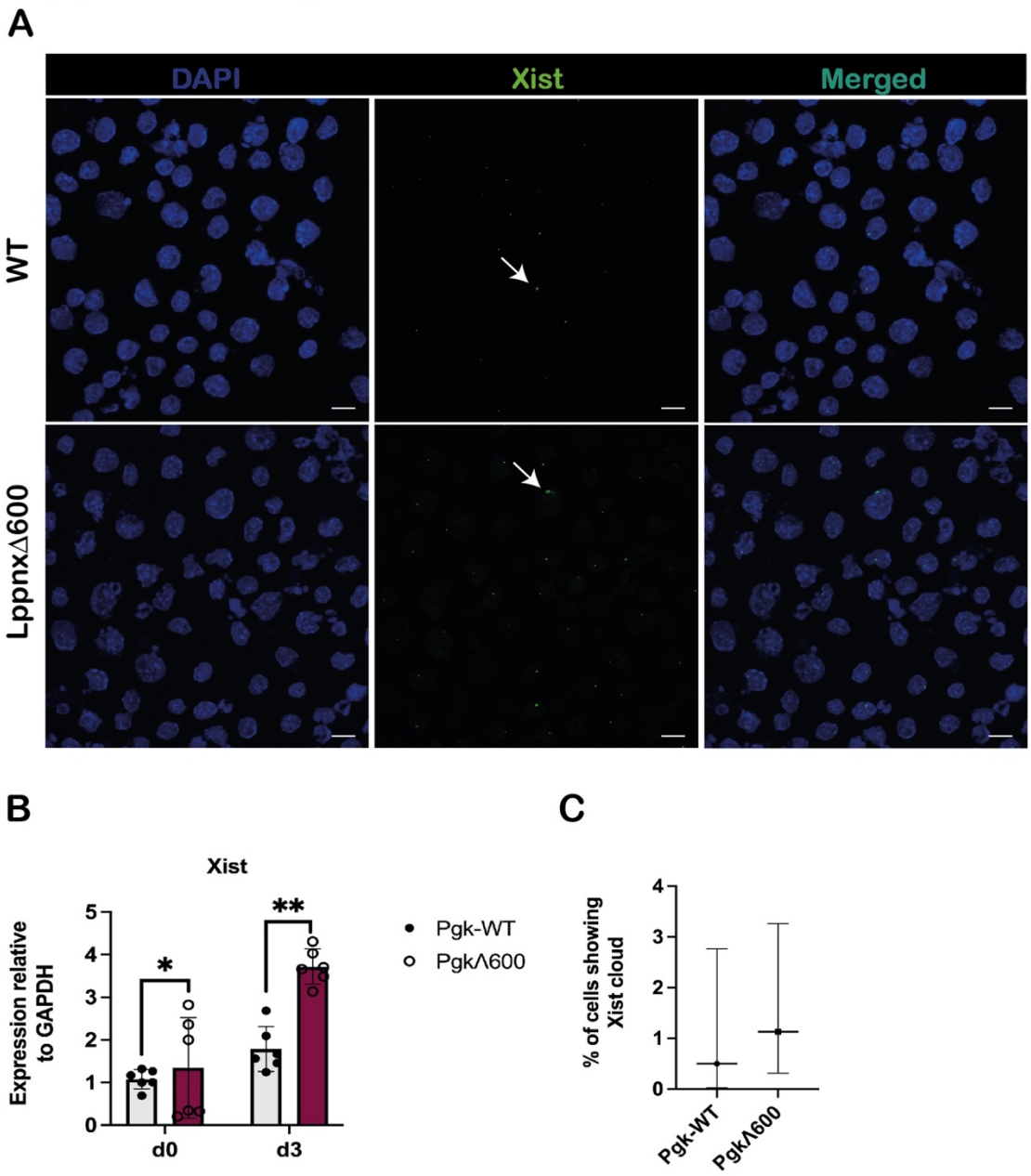

Fig. S3. Genetic ablation of the Lppnx promoter region in Pgk1a male ES cells shows only a mild effect. Male ES cells were generated either from WT Pgk1 mice or from Pgk1 mice carrying the 600bp deletion of Lppnx. RNA-FISH was carried out on these cells after differentiation to analyse the number of XIST clouds formed. Scale bar: 10µm (A). qRT-PCR for Xist of WT and LppnxΔ600 ES cells shows a slight increase of Xist transcription in mutant ES cells Two-sample t-test Pgk-WT: p=0.0193, Pgk Δ600: p=0.0032 (B). Quantification of the number of Xist foci in percent from the experiment shown in (A). Mutant ES cells exhibit a slightly increased number of Xist clouds after differentiation. Percentages are given with an upper and lower lever and are calculated with a confidence interval of 95% (Wilson/Brown) (C).

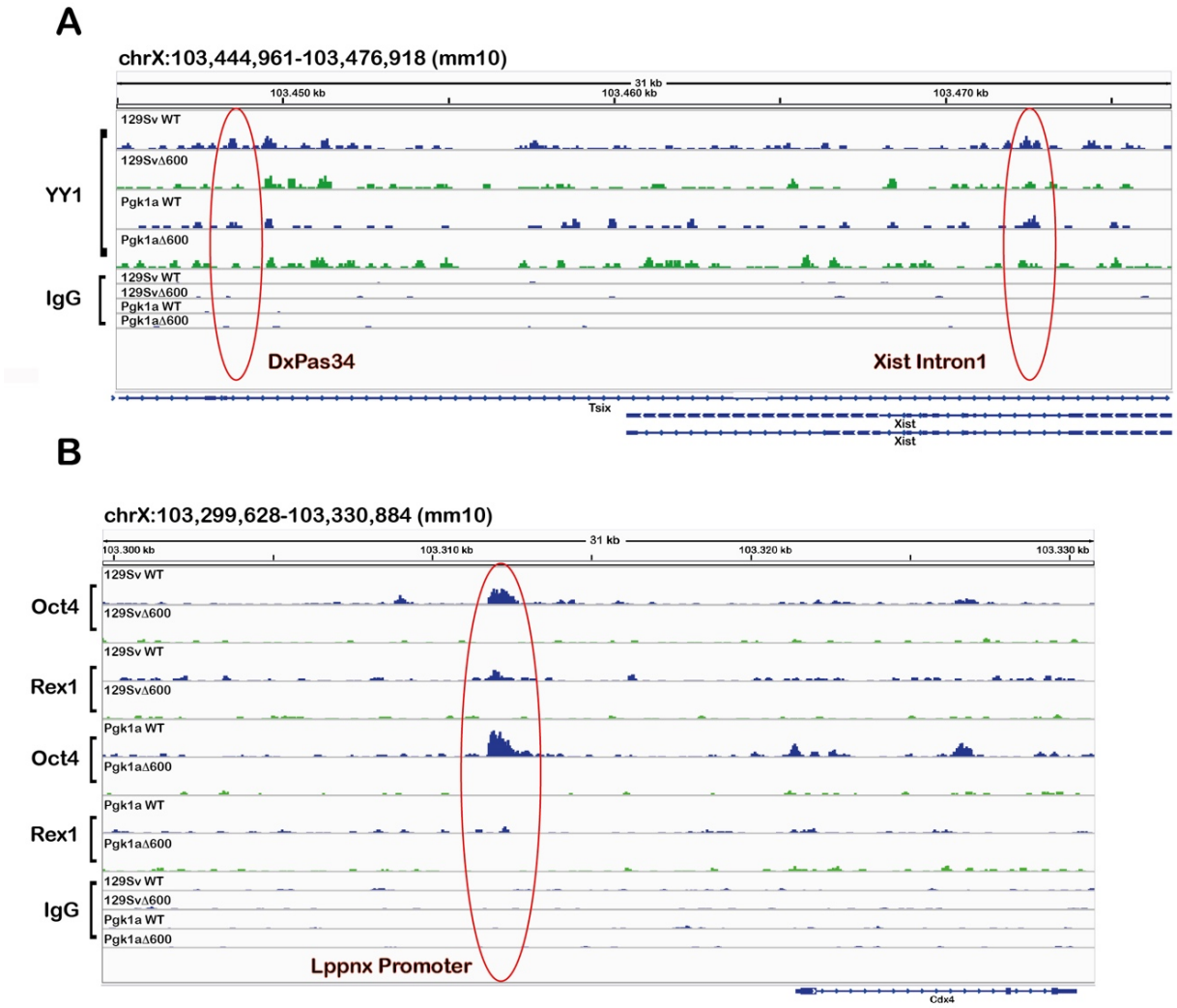

Fig. S4. Ablation of Lppnx does not affect the binding of YY1 in XI1 and DxPas34. ChIPseq experiments show no alteration in YY1 binding in the two key regions XI1 and DxPas34 in male 129Sv and Pgk1a ES cells (A). Differential loading of Oct4 and Rex1 on the Lppnx promoter region suggests differential expression levels in male 129Sv and Pgk1a ES cells (B).

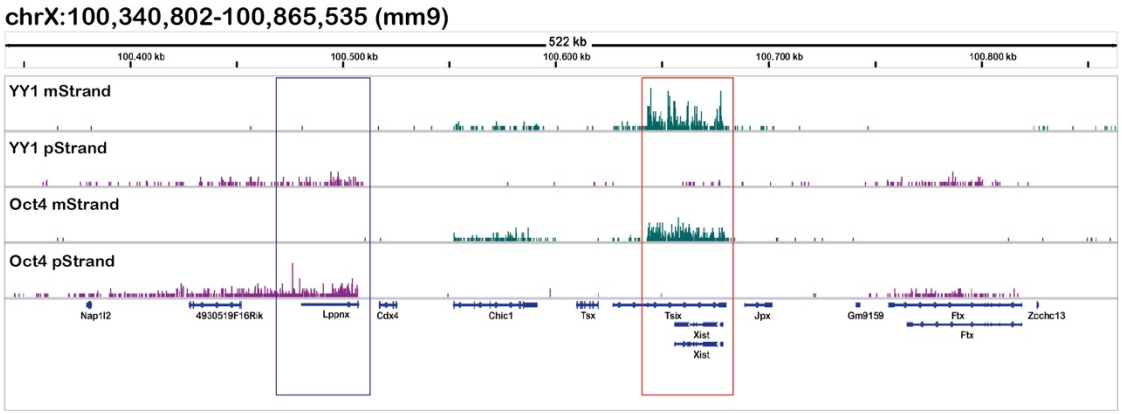

Fig. S5. Oct4 binds to Lppnx and Tsix lncRNAs. CLIP-Seq data show that Lppnx (pStrand) binds to Oct4 and to a lesser extent to YY1. The Lppnx core region is marked with a blue box. Both, YY1 and Oct4 bind in similar strength to Tsix (mStrand, red box).

.

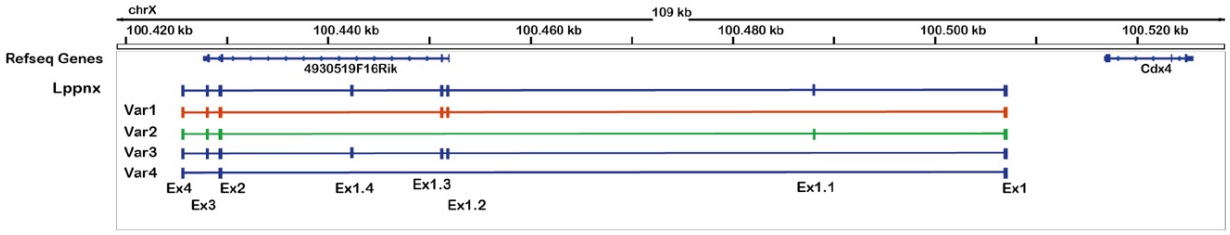

Fig. S6. Lppnx expression occurs in different splice variants in Xcea and Xcec ES cells. Position and splice variants of Lppnx obtained by 3Prime RACE. Var1 was found predominantly in Xce^{a} cells whereas Var2 is expressed in Xce^{c} ES cells. Var3 and 4 were found equally in both cell types.

SI Methods

Single-cell gene expression analysis

Hybrid ES cells were sorted by fluorescence-activated cell sorting using the MoFlo system (Beckman Coulter, Brea, CA, USA), and individual cells were distributed into wells of 96-well plates containing 5 µl of Cells Direct resuspension buffer (Invitrogen, Carlsbad, CA, USA). The preamplification step consisted of 20 cycles using a mix of universal primer pairs to pre-amplify each gene simultaneously. Preamplification was followed by exonuclease I treatment (New England Biolabs, Ipswich, MA, USA), and allelic qPCR which was performed using a BioMark thermal cycler (Fluidigm). Raw efficiencies of each PCR assay and allelic specificity were measured on control genomic DNA within each experiment. Ct values for a given gDNA sample were: 23,39190544 for 129Sv and 23,04471168 for the Pgk allele. Transcript levels were extrapolated using the raw PCR efficiencies, thus allowing the direct comparison of different genes. Primer sequences are given in the Supplementary Table.

Chromatin immunoprecipitation and sequencing (ChIP-Seq)

Cells were harvested with accutase, counted and centrifuged at 600 g for 3 min. Pellets were then washed three times in 1.5 ml Wash Buffer (20 mM HEPES pH 7.5; 150 mM NaCl; 0.5 mM Spermidine; 1X protease inhibitors EDTA-free) and resuspended in Wash Buffer to a density of 500000 cells per 100ul. 100ul of the cell suspension was then transferred into an 8-stripe tube containing 10ul of previously activated concanavalin A coated magnetic beads (activating buffer: 20mM HEPES pH 7.5, 10mM KCl, 1mM CaCl2, 1mM MnCl2) (86057-3, BioMag®Plus Concanavalin A, Generon) and placed in a rotator for 10 minutes at room temperature. Cells were resuspended in 50µl Antibody Buffer (5% (wt/vol) digitonin, 20 mM HEPES pH 7.5; 150 mM NaCl; 0.5 mM Spermidine; 1X protease inhibitors EDTA-free, 2mM EDTA) and 0,5 µl antibody was added per sample and incubated at 4°C overnight in a rotator. The following antibodies were used: Oct4 (abcam #ab19857), Rex1 (Novus #NBP1-31948), YY1 (abcam #ab38422) and IgG. (Diagenode #C152 000 01). Cells were washed 3 x in 250ul Dig-wash Buffer (5% (wt/vol) digitonin, 20 mM HEPES pH 7.5; 150 mM NaCl; 0.5 mM Spermidine; 1X protease inhibitors EDTA-free) to remove unbound antibody. Cells were resuspended in 50 µl cold Dig-wash Buffer and pAG-MNase 1:200 was added and incubation continued at room temperature for a further 10 minutes. At this stage, supernatant from samples incubated with IgG antibody was collected and stored to be used as input. Cells were washed 3 x in 250ul cold Dig-wash Buffer to remove unbound pAG-MNase. Tubes were placed on ice and quickly mixed with 100 mM CaCl2 to a final concentration of 2 mM diluted in 50ul Dig-wash buffer per sample. Cells were incubated for 2h at 4ºC and the reaction was quenched by the addition of 33ul 2X STOP BUFFER (340mM NaCl; 20mM 0.5 EDTA; 4mM EGTA; 0.05% digitonin; 100ug/mL RNAse A; 50ug/mL Glycogen). Cleaved fragments were liberated into the supernatant by incubating the cells at 37°C for 10 minutes, and the supernatant stored. DNA fragments were purified from the supernatant using the ChIP DNA Clean and Concentrator Kit (D5205, Zymo Research) and used for the construction of sequencing libraries.

Generation of Lppnx KO mice

To generate a transgenic mouse line with the promoter of Lppnx deleted we used CRISPR (clustered regularly interspaced short palindromic repeats)-Cas9 to target this region in the mouse zygote. Briefly, crRNAs targeting this genomic region with minimal off target potential were identified (crRNA-1 GGT-TTTTGCTCCTTGAGCTTCT and crRNA-2 CAGACCCATGGAAGCTCCC-TGG). S. pyogenes Cas9 nuclease activity at these crRNAs cut sites would result in a 595bp deletion. spCas9 protein, crRNAs and the universal tracrRNA required to form a functional gRNA were all purchased from Integrated DNA Technologies, Inc. (IDT). An asymmetric single stranded DNA (ssDNA) repair template was designed across the proposed deleted region, containing homology arms 90bp upstream and 40bp downstream from the targeted cut sites (IDT). Silent shield mutations for both gRNAs were integrated to prevent cutting of the repair template. A microinjection mix containing the annealed gRNA complexes (20ng/ul each), Cas9 protein (20ng/ul) and the ssDNA repair template (10ng/ul) was prepared and directly microinjected into C57BL/6J, 129Sv/Pas or 129Hprt^{bm1}Pgk1a zygote pronuclei using standard protocols. Zygotes were cultured overnight and the resulting 2 cell embryos surgically implanted into the oviduct of day 0.5 post-coitum pseudopregnant mice. Potential founder mice were screened by PCR using primer Ahi112 and Ahi113 for the required deletion and positive animals fully verified by Sanger sequencing. A founder mouse containing a 592bp deletion between the two crRNAs cut sites was selected and back-crossed to wild-type mice to confirm germline penetrance.

Supplementary Table. Sequence of primer used in this study

Primer	Sequence	Figure	Purpose
AHi135	CCCCAGGAAGTGCAAATGTT	S2	Detection of 129Sv derived Lppnx RNA by qRT-PCR
AHi136	CCCCAGGAAATGCAAATGTA	S2	Detection of Pgk1a derived Lppnx RNA by qRT-PCR
AHi137	TGGTGGTACCGCTCAACTG	1	Detection of Lppnx RNA by qRT-PCR
AHi138	GTGGTTCTAATTCCCTCAAGGAT	1	Detection of Lppnx RNA by qRT-PCR
AHi146	TGCGACTTCAACAGCAACTC	1,2,3,4,5,S3	GAPDH Normalization for qRT-PCR
AHi147	GCCTCTCTTGCTCAGTGTCC	1,2,3,4,5,S3	GAPDH Normalization for qRT-PCR
AHi112	GAATGGGATGGGGCAGTTGT	2	Detection of the 600bp Deletion of the Lppnx promoter
AHi113	TGGCCTCTTGCTTCTTCGTG	2	Detection of the 600bp Deletion of the Lppnx promoter
AHi135	CCCCAGGAAGTGCAAATGTT	2	Detection of 129Sv derived Lppnx RNA by qRT-PCR
AHi136	CCCCAGGAAATGCAAATGTA	2	Detection of Pgk1a derived Lppnx RNA by qRT-PCR
AHi209	GTTGGAGAAGGTGGAACCAA	2	Detection of Oct4 mRNA by qRT-PCT
AHi210	CTCCTTCTGCAGGGCTTTC	2	Detection of Oct4 mRNA by qRT-PCT
AHi211	TCTTCTCTCAATAGAGTGAGTGTGC	2	Detection of Rex1 mRNA by qRT-PCT
AHi212	GCTTTCTTCTGTGTGCAGGA	2	Detection of Rex1 mRNA by qRT-PCT
AHi170	TTCTTTCCCCAGATCTTGCAC	2	Detection of Rnf12 mRNA by qRT-PCT
AHi172	TGTCTAATGCACAGTAACAGTGTTGT	2	Detection of Rnf12 mRNA by qRT-PCT
AHi244	GGTTCTCTCTCCAGAAGCTAGGAAAG	2,3,5	Detection of 129Sv derived Xist RNA by qRT-PCR
AHi248	TGGTAGATGGCATTGTGTATTATATGG	2,3,5	Detection of 129Sv derived Xist RNA by qRT-PCR
AHi239	CTCCTGTGACAGCCTTTCTGAAG	2,3	Detection of Nestin mRNA by qRT-PCT
AHi240	AGGATAGGGAGCCTCAGACATAGG	2,3	Detection of Nestin mRNA by qRT-PCT
AHi394	CACCGgaaagctgcaggcccagcc	3	Generation for sgRNA 80kb deletion 5Prime
AHi395	AAACggctgggcctgcagctttC	3	Generation for sgRNA 80kb deletion 5Prime
AHi396	CACCGtatcattgtattgaggacc	3	Generation for sgRNA 80kb deletion 3Prime
AHi397	AAACggtcctcaatacaatgataC	3	Generation for sgRNA 80kb deletion 3Prime
AHi398	CACCGcagacccatggaagctccc	3	Generation for sgRNA 72kb deletion 5Prime
AHi399	AAACgggagcttccatgggtctgC	3	Generation for sgRNA 72kb deletion 5Prime
AHi116	ACGTTCAGGGGGAAGACTAA	3	Detection of the 80kb deletion
AHi117	ATATGGGATTAATTTCCAAAACACA	3	Detection of the 80kb and 72kb deletion
AHi110	CAGTGAATCCGCCCAACCTT	3	Detection of the 72kb deletion
AHi211	TCTTCTCTCAATAGAGTGAGTGTGC	4	Detection of Rex1 mRNA by qRT-PCT
AHi212	GCTTTCTTCTGTGTGCAGGA	4	Detection of Rex1 mRNA by qRT-PCT
AHi245	GGTTCTCTCTCCAGAAGCTAGGAGAA	4,S3	Detection of Pgk1a derived Xist RNA by qRT-PCR
AHi173	GAGGGGAAGGGTTAGCATTTG	4	Detection of 129Sv derived Chic1 RNA by qRT-PCR
AHi174	TGGTGGACTTTGTCAGGTTAGCA	4	Detection of Pgk1a derived Chic1 RNA by qRT-PCR
AHi175	TGACAGGTGATAGTTTTCTCGTTACTTT	4	Detection of Pgk1a and 129Sv derived Chic1 RNA by qRT-PCR
AHi66	GAGAGTCCAGAGCGACCCaTc	4	Detection of 129Sv derived Pgk1 RNA by qRT-PCR
AHi67	GAGAGTCCAGAGCGACCCaTt	4	Detection of Pgk1a derived Pgk1 RNA by qRT-PCR
AHi69	CCATTCCACCACCAATGATC	4	Detection of Pgk1a and 129Sv derived Pgk1 RNA by qRT-PCR
AHi372	CACCGTGTGTGATGGCACCTCCTAA	5	Generation for sgRNA Xist Intron1 deletion 5Prime
AHi373	AAACTTAGGAGGTGCCATCACACAC	5	Generation for sgRNA Xist Intron1 deletion 5Prime
AHi374	CACCGTTCTGCCCAGAACAGACCAC	5	Generation for sgRNA Xist Intron1 deletion 3Prime
AHi375	AAACGTGGTCTGTTCTGGGCAGAAC	5	Generation for sgRNA Xist Intron1 deletion 3Prime
AHi376	CTGAAGATGGTGATGGCGAGT	5	Detection of the deletion of Xist intron1
AHi377	ACGCCAAGGGTAGCAAGAGA	5	Detection of the deletion of Xist intron1